

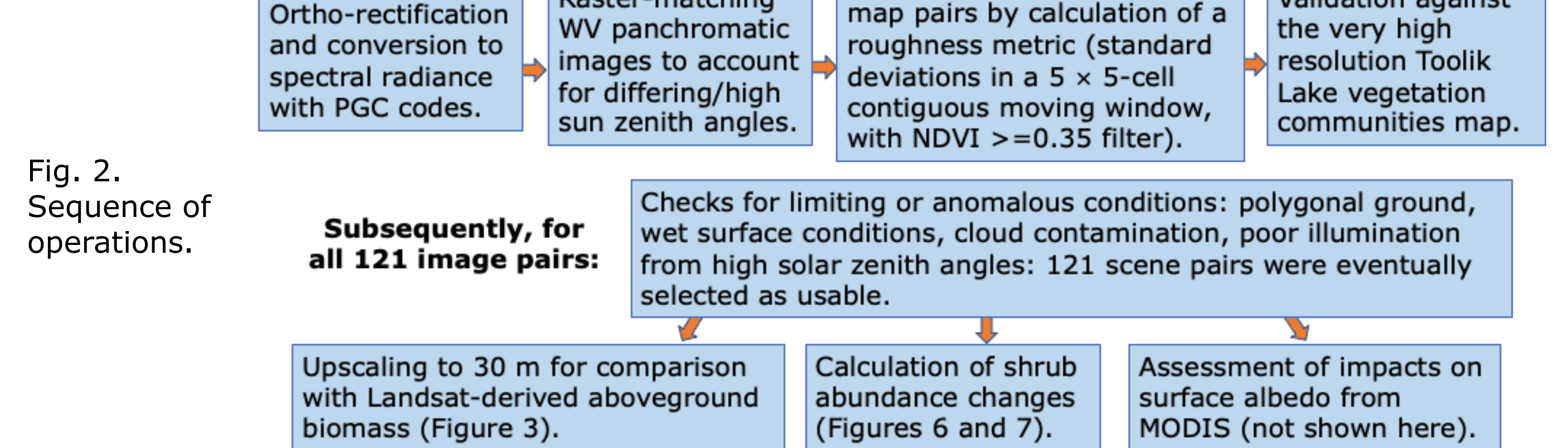
Mapping Shrub Abundance in Arctic Tundra from the Satellite High Resolution Record and Impacts on Albedo: Validation

Mark Chopping¹, Darko Radakovic¹, Angela Erb², Rocio Duchesne³, Zhuosen Wang⁴, and Crystal Schaaf²

¹ Montclair State University ² University of Massachusetts, Boston ³ University of Wisconsin Whitewater ⁴ University of Maryland College Park, Earth System Science Interdisciplinary Center

Overview The goal is to map shrub abundance and cover at high spatial resolution (2.5 m) and quantify error in the cover estimates so that change can be reliably detected. Maps were created for 127 sites of 2 km × 2 km in Alaskan Arctic tundra, with early/late QuickBird-2/WorldView-2/3 panchromatic and NDVI image pairs, over a 15- to 18-year period, to provide a dataset that can be used to assess the impact on summer surface albedo, inform modeling studies, and validate lower spatial resolution ABoVE data products. Validation was effected using the 'Vegetation Community Maps for the Toolik Lake Area, 2013-2015' (Greaves et al. 2018); and results for a series of sites where imagery is available for multiple years. **Imagery** The high spatial resolution images included QuickBird (~0.6 m) ca. 2005 and Worldview-2 (~0.5 m) and Worldview-3 (~0.3 m) from 2015 - 2021, to form early/late period image pairs for diverse cloud free summer tundra landscapes (Fig. 1). All imagery was orthorectified to the ABoVE Albers Conic Equal Area grid at 0.5 m using ArcticDEM (Porter et al. 2018) and simultaneously converted to calibrated spectral radiances using the Polar Geospatial Center pgc_ortho.py code.

Mapping Approach A generalization of the CANAPI approach (Chopping 2011) was used to delimit the extent and abundance of shrubs.



Validation I The Toolik Lake Vegetation Community Map was reprojected onto the same 2.5 m. The classes 0_No_Data, 5_Low dense shrub, 8_Shrubby tussock tundra, 10_Shrubby moist non-tussock tundra, 11_Low to tall moist shrub, and 12_Tall shrub were recoded 0_No_Data → 0; 5 & 8 → 1; 10 & 11 → 2; and 12 → 3. The 2009 and 2017 maps were recoded to the classes 'none', 'sparse', 'moderate', and 'tall', with <1.1, 1.1<1.5, 1.5<3, and >=3. All maps were masked for a small region of invalid imagery before calculation of confusion matrices and the overall/user's, producer's accuracies (Table 1).

Validation II In order to quantify error and assess the impacts of using imagery acquired at differing solar and viewing angles, all available panchromatic images were processed for a subset of sites, using Yen thresholding (Yen et al. 1995) to obtain shrub canopy extents.

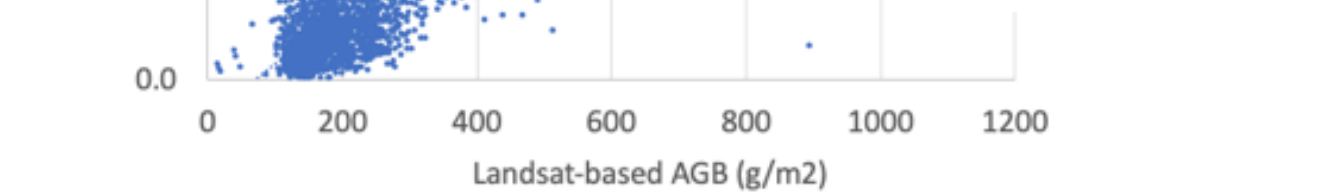


Fig. 3. Image roughness metric from an orthorectified QuickBird panchromatic image averaged over 30 m pixels, as a function of Landsat-based shrub aboveground biomass (AGB; g/m²) from Berner et al. 2018, for a 2 x 2 km site on the Colville River, Alaska.



TABLE 1. CONFUSION MATRICES & ACCURACY VS TOOLIK LAKE MAP

	QuickBird-2	Not Shrub	Sparse	Moderate	Tall shrub	User's	Producer's
QuickBird-2							
Not Shrub	82.5	65.9	51.6	46.1	0.77	0.82	
Sparse shrub	10.2	19.9	19.0	8.4	0.55	0.20	
Moderate shrub	6.5	13.2	24.2	28.5	0.44	0.24	
Tall shrub	0.8	1.0	5.2	17.0	0.32	0.17	
WorldView-2							
Not Shrub	76.3	62.2	41.5	37.0	0.78	0.76	
Sparse shrub	13.7	22.6	23.1	8.8	0.59	0.23	
Moderate shrub	9.2	14.5	31.2	38.4	0.48	0.31	
Tall shrub	0.8	0.7	4.2	15.8	0.37	0.16	

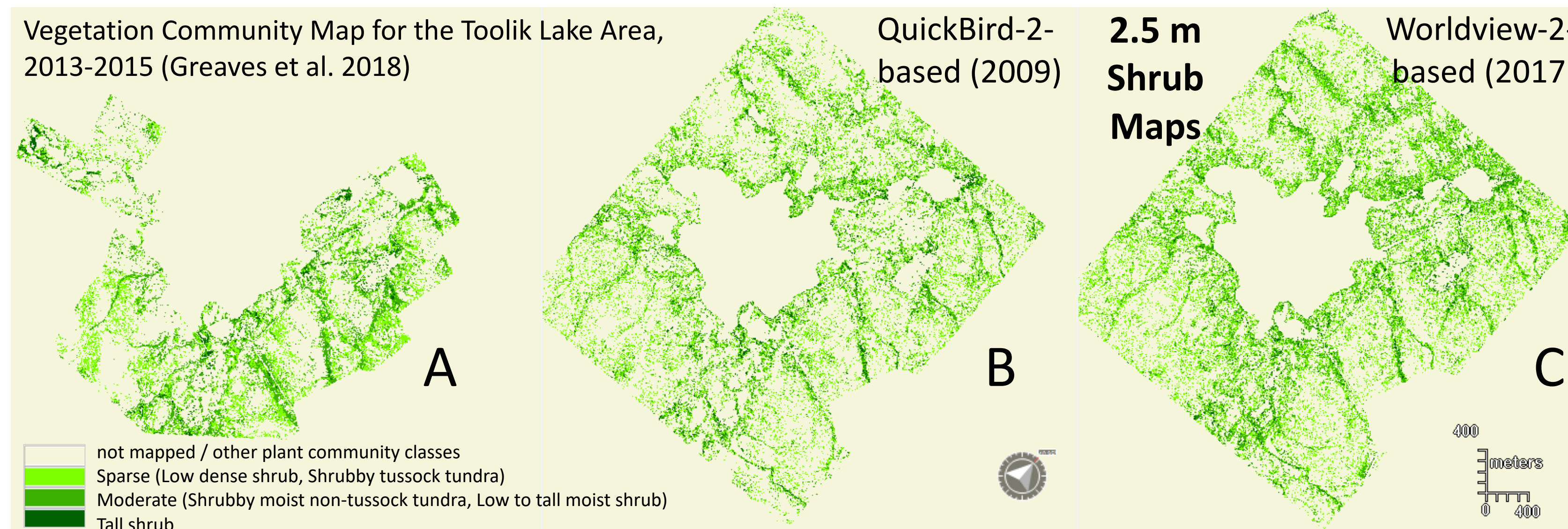


Fig. 4. Toolik Lake ABoVE Sentinel site in Alaska (a) shrub class of the Vegetation Community Map, Toolik Lake Area, 2013-2015 (Greaves et al. 2018) (b) mapped shrub classes derived from panchromatic image roughness based on QuickBird (QB), July 18, 2009 (QB021500009JUL18220421-P1BS-500071841070_01_P001) (c) the same, from WorldView-2 (WV02), August 11, 2017 (WV02_20160612215015_1030010057A6E600_16JUN12215015-P1BS-501511474060_01_P012).

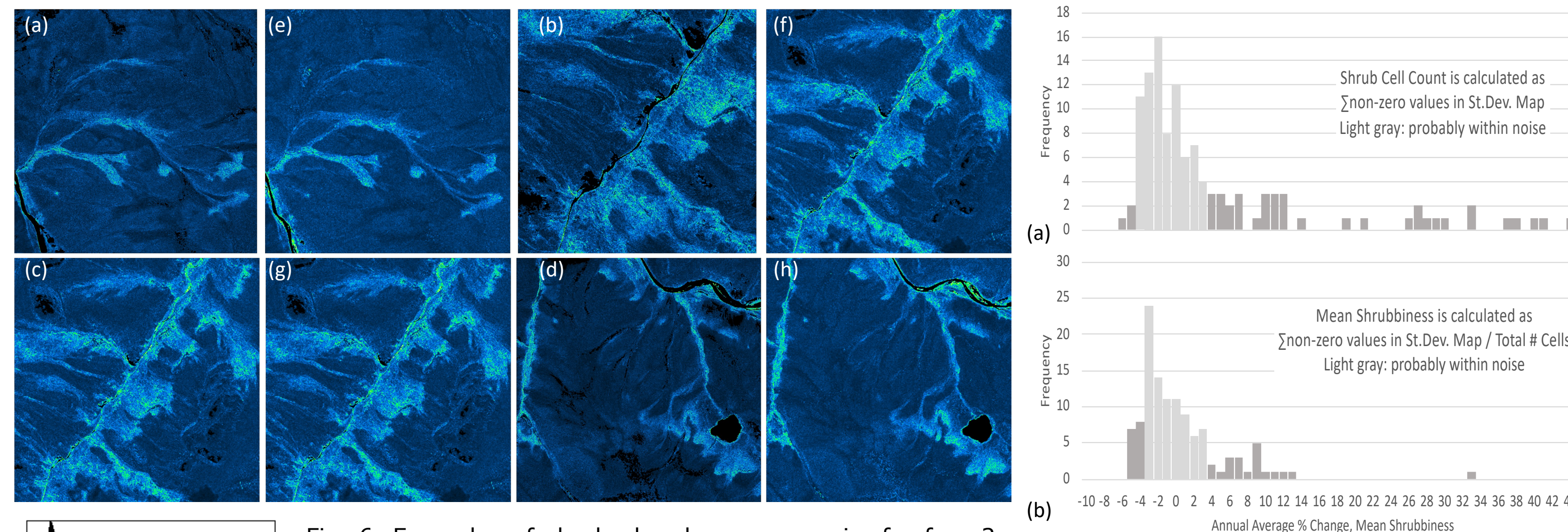


Fig. 5. Examples of shrub abundance map pairs for four 2 km² areas in Project Site 01, North Slope of Alaska (a)-(d) 24 JUL 2005 map (QB02) (e)-(h) 16 JUL 2020 map (WV02). Mapped shrubs were limited to the areas shown using the "Moments" auto-thresholding algorithm (Tsai 1985).

Many cover sequences show anomalous, often infeasible trajectories (Fig. 5), usually traceable to low sun elevation or high viewing angles in the WV02 imagery, or sometimes other factors such as cloud, cloud shadows, or polygonal ground. The set of 115 cases was filtered to 110 by removing cases that showed infeasible rates of change, using: invalid if (abs(cover_cover_LastValid) / (time-time_LastValid) > 2.4 and (time difference > six months)). This generated 108 cases with N>1. Investigation of one site with an apparently anomalous -but not infeasible- reveals the impact of low sun angles: with 9.8° vs 34.2°, the distribution is more sparse (Fig. 8), though the relationship is not systematic across all cases: multiple regression of cover on sun and view angles yielded an adjusted R²=0.04, N=789, significant at p=0.05, indicating a weak dependence.

Results, Validation I - The overall, user's, and producer's accuracies were 64%, 77%, and 82%, respectively, for the QB-derived map; and 61%, 78%, and 76%, respectively, for the WV-derived map. If classes are combined to none/sparse and moderate/tall, the accuracies are 82%, 87%, and 92% (QB); and 81%, 88%, and 89% (WV; Table 1). Shrub cover was calculated as 11.4% and 14.5% in 2009 and 2017, respectively, though this may partly reflect the higher intrinsic spatial resolution of WorldView vs QuickBird images rather than real change; if so, the rate of 0.39/year can be used to correct change estimates for all 121 sites with usable pairs (Fig. 6). **Validation II** - Trajectories of shrub cover estimates have limited precision, even after filtering for infeasible rates of change; there is still noise of a similar or greater magnitude than the expected change (Figs 5, 9). Of the 108 cases, 34 showed a decrease, 17 almost no change; and 57 an increase, with mean changes of 0.18 in slope values of either sign (Fig.10). **Findings:** High resolution maps of shrub abundance generated using a roughness metric on panchromatic imagery are strongly related to aboveground biomass determined from 30 m Landsat imagery (Berner et al. 2018.; Fig. 3) and highly compatible with shrub distributions seen in very high resolution plant community maps (Greaves et al. 2018; Fig. 4, Table 1). The impact of image spatial resolution was quantified. Although the approach described generates

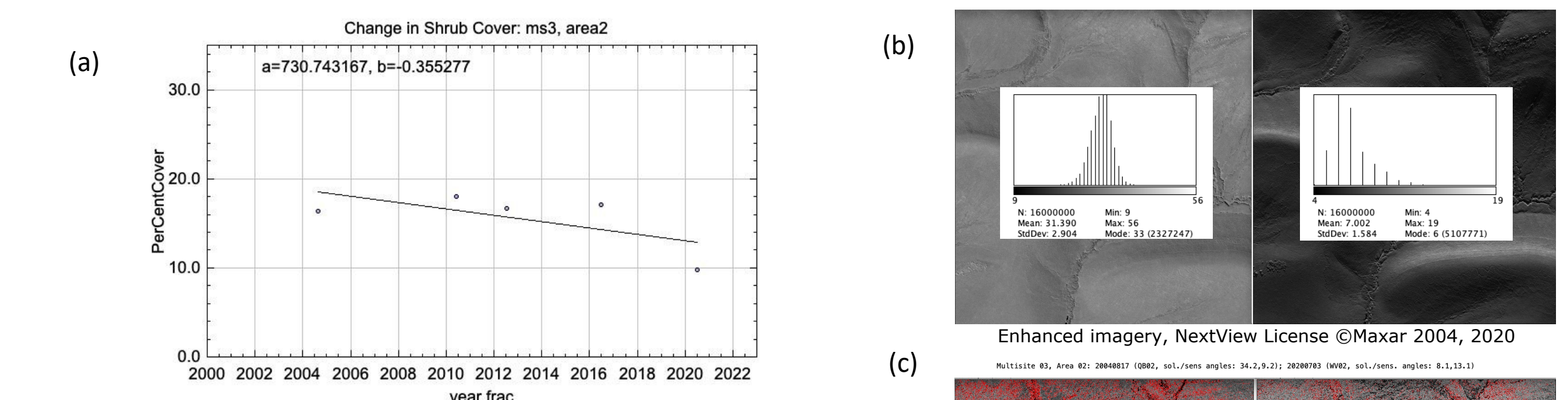


Fig. 8. (a) Estimated shrub cover for site 3, area 2 (LL: 151.791353°W, 69.049942°N). The 2004 estimate was derived from QB02 panchromatic imagery; the remaining estimates are derived from WV02 panchromatic imagery (b) enhanced pan images for 2004 and 2020, acquired at solar elevation angles of 34.2 and 9.8°, respectively. (c) shrub canopy detected using Yen auto-thresholding, in red.

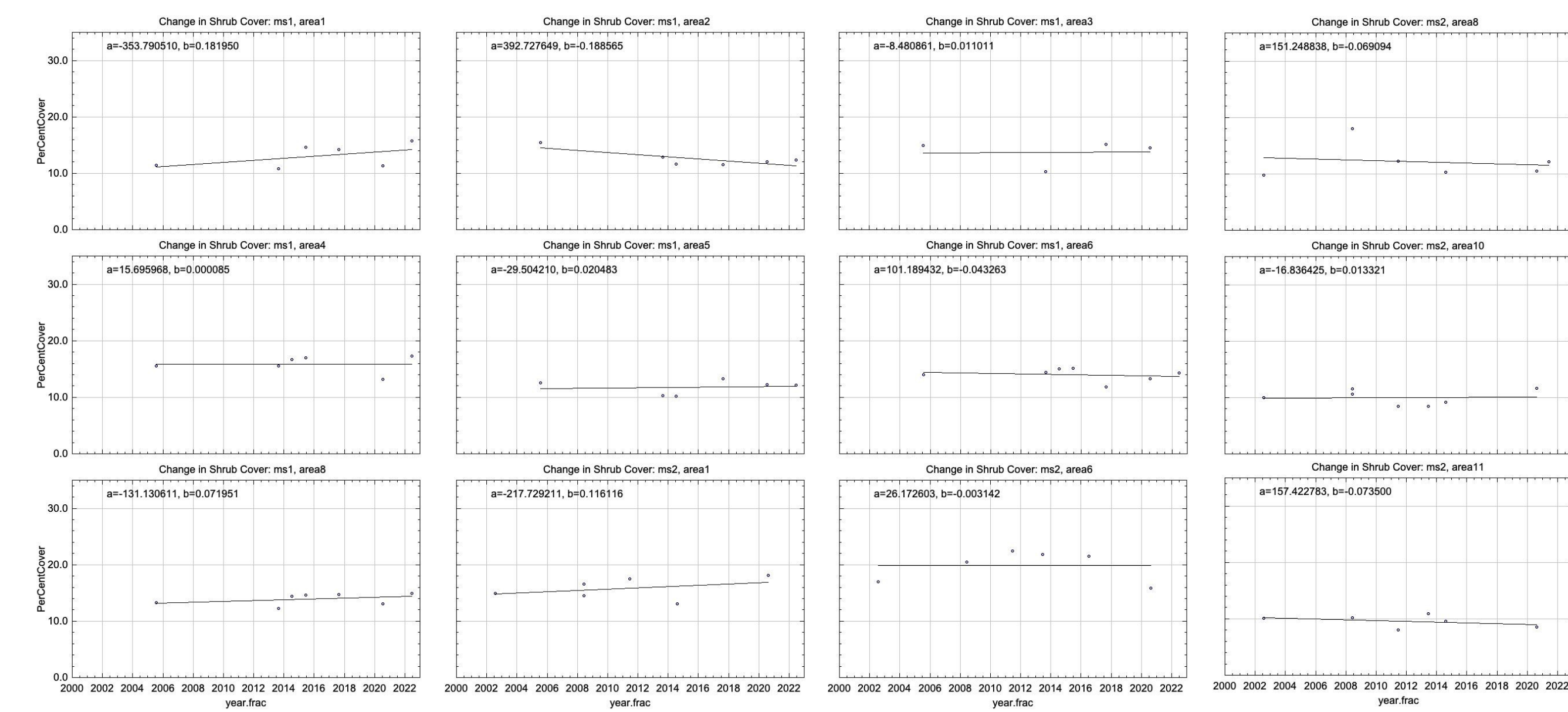


Fig. 9. (a) Estimated shrub cover trajectories for various sites. The 2004 estimate was derived from QB02 panchromatic imagery; the remaining estimates are derived from WV02 panchromatic imagery.

estimates that are consistent with Landsat-based AGB, both methods are known to be inaccurate over polygonal ground with non-shrub vegetation in troughs, for different reasons (respectively: because imagery roughness at this scale is enhanced importantly; and because spectral measures appear similar for shrub and locations where there is relatively lush and abundant non-shrub vegetation cover, e.g., in the troughs where water collects). Lack of precision in estimates is reflected in their trajectories, which are often non-monotonic. This is expected: the distribution of variance in cover estimates acquired in the same month - one way to estimate measurement error - is heavily skewed towards lower values, with a mean standard deviation across all cases of 5.57, with 62% of cases less than 4 (N=58).

Future Work: Annual % change in shrub abundance outside probable noise (±3%) indicates increased shrub size and abundance (Fig. 7), but the precision of change estimates is limited. Future work will seek to improve precision by leveraging machine learning approaches; see the poster by Radakovic et al.,

Acknowledgments: This work was supported by award NNX15AU08A to MC. We gratefully acknowledge Maxar and the National Geospatial-Intelligence Agency for access to imagery and the assistance of the NASA, GSFC NCCS User Services Group; Liz Hoy (ABoVE Science Cloud Lead, NASA, GSFC); Mark Carroll (NASA, GSFC); Clare Porter (Polar Geospatial Center); and Wayne Rasband (National Institutes of Health).

References
 Berner, L.T., P. Jantz, K.D. Tape, and S.J. Goetz, 2018. ABoVE: Gridded 30-m Aboveground Biomass, Shrub Dominance, North Slope, AK, 2007-2016. ORNL DAAC, Oak Ridge, Tennessee, USA. <https://doi.org/10.3334/ORNLDAAC/1565>.
 Chopping, M., 2011. CANAPI: Canopy Analysis with Panchromatic Imagery, *Remote Sensing Letters* 2(1): 21-29.
 Greaves, H.E., L. Vierling, J. Eitel, N. Boelman, T. Magney, C. Prager, and K. Griffin, 2018. High-Resolution Shrub Biomass and Uncertainty Maps, Toolik Lake Area, Alaska, 2013. ORNL DAAC, Oak Ridge, Tennessee, USA. <https://doi.org/10.3334/ORNLDAAC/1573>.
 Porter, C., et al., 2018. ArcticDEM, Version 3, <https://doi.org/10.7910/DVN/OHUKH>, Harvard Dataverse, V1, last access: summer 2022.
 Tsai, W., 1985. *Computer Vision, Graphics, and Image Processing*. Moment-preserving thresholding: a new approach., 29, 377-393.
 Yen, J.-C., Chang, F.-J & S. Chang, 1995. A new criterion for automatic multilevel thresholding. *IEEE Transactions on Image Processing*, 4(3), 370-378. doi:10.1109/83.36647